Temperature-dependent surface structure and lattice dynamics of NiO(001)

T. Okazawa, Y. Nakagawa, and Y. Kido*
Department of Physics, Ritsumeikan University, Kusatsu, Shiga-ken 525-8577, Japan
(Received 23 October 2003; published 19 March 2004)

Temperature-dependent surface relaxation and rumpling of NiO(001) were determined by high-resolution medium energy ion scattering. We found that the top-layer Ni plane is displaced toward the vacuum side relative to the top-layer O plane at temperature below 420 K. This is consistent with the *ab initio* calculation but contradicts the shell model calculation using pair potentials. However, at a temperature above 500 K (close to the Néel temperature), relative positions of the O plane to the Ni plane in the top and second layers are reversed. This result suggests that the surface structure is very sensitive to even a slight change of the bulk lattice. We also measured temperature dependent bulk and enhanced thermal vibrations (TVAs) of the top-layer atoms. The Debye temperatures for Ni and O estimated from the bulk TVAs of Ni and O using the simple Debye model are consistent with those derived from the heat capacity measurement. The bulk TVA gradually increases with increasing temperature, while the enhancement of the TVA of the top-layer Ni in the surface normal direction suddenly drops at 500 K. Such a dramatic change may be related to the reversal of the rumpling of the top layer. In contrast to alkali halide crystals, there are no correlations between the first nearest neighbor atoms in the [001] and [101] strings. The present result claims that pair potentials are not applicable to the NiO crystal which has, in part, covalent bonding.

DOI: 10.1103/PhysRevB.69.125412 PACS number(s): 68.35.Ja, 63.20.−e

I. INTRODUCTION

Nickel monoxide (NiO) is a charge transfer type insulator with strongly correlated *d* electrons. As is well known, NiO is an antiferromagnet with a Néel temperature of 523.6 K. A second order phase transition occurs from a rhombohedral to a cubic structure (NaCl type). Its bulk and surface electronic properties have been recently investigated by photoelectron, metastable He atom diffraction, and scanning tunneling microscopy[1–6] and also theoretically by an *ab initio* calculation based on the local spin density approximation.[7] Recently, lattice-dynamical calculations using density-functional perturbation theory (DFPT) has been applied to metals, semiconductors, and some oxides.[8] The phonon dispersion relations calculated along some high-symmetry lines in the first Brillouin zone agree well with experimental ones determined by neutron scattering.[9] In order to calculate thermal vibration amplitudes (TVAs), however, one must solve the equations of motion for all the wave vectors in the first Brillouin zone and average the amplitudes over all the wave vectors combined with the Planck distribution function. This requires very long computing times. For a more precise calculation using DFTP at a finite temperature, an *ab initio* molecular dynamics (MD) simulation should be performed using a supercell containing a relatively small number of atoms and periodic boundary condition. Its accuracy depends on the size of the supercell. A recent high-resolution ion scattering analysis makes it possible to determine directly average TVAs of near surface atoms with good accuracies.[10,11] Reliable data on thermal lattice vibrations would stimulate and further develop the full quantum mechanical calculations to be applied to the dynamics of solid surfaces.

In previous work,[12] we determined the rumpled surface structure and root mean square (rms) TVAs of NiO(001) at room temperature (RT) by high-resolution medium energy ion scattering (MEIS). In contrast to alkali halide crystals, it was found that the top-layer cation (Ni^{2+}) plane was displaced toward the vacuum side relative to the top-layer anion (O^{2-}) plane. This is consistent with an *ab initio* calculation based on the density functional theory using the local spin density approximation.[13]

As mentioned above, the crystal structure changes from a rhombohedral to a cubic lattice at a Néel temperature of 523.6 K. Up to now, there have been some reports on the anomaly of the bulk specific heat of NiO at the Néel temperature.[14,15] We can expect that a slight change of the bulk structure may significantly affect the surface structure and lattice dynamics. So it is interesting to study the temperature dependence of the displacements and enhanced thermal vibrations of near surface atoms around the Néel temperature. In a previous experiment,[12] we determined the vertical positions of the top-layer Ni- and O-planes scaled from the second-layer Ni plane. In this study, adopting appropriate double alignment geometries reduces background levels and makes it possible to determine the temperature dependent vertical displacements of the top- and second-layer Ni and O planes scaled from the third-layer Ni planes. Furthermore, the scattering yields from the second-layer and deeper layer Ni atoms for various kinds of scattering geometries derive the TVAs of the bulk and near-surface atoms at temperatures from RT up to 650 K.

II. EXPERIMENT

Single crystal rods of NiO(001) with a purity of better than 99.93% were purchased from Earth Chemical Company. The sample piece was prepared by cleavage in a dry N_2 ambient and then immediately introduced into an ultrahigh vacuum chamber. Annealing at 770 K for 40 min in a O_2 pressure of 1×10^{-4} Torr leads to a clean 1×1 surface, which was observed by reflection high energy electron diffraction (RHEED). Auger electron spectroscopy confirmed

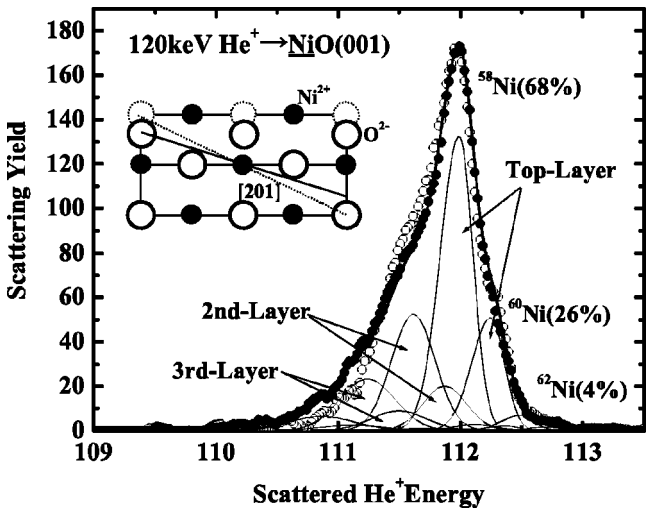

FIG. 1. MEIS spectra observed for 120-keV He^+ ions incident along the [201] axis (open circles) and $+1.0°$ off from this axis (full circles) and backscattered from Ni atoms of NiO(001) at RT. The scattering angle is fixed to 60.3°, and the scattering plane is (010).

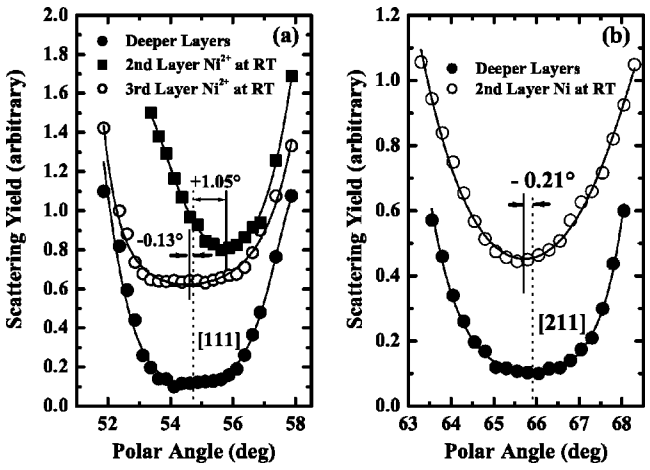

FIG. 2. (a) Polar scan spectra around the [111] axis in the (110) plane for the scattering components from the second (full squares), third (open circles), and deeper layers (full circles) Ni atoms. (b) Polar scan spectra around the [211] axis in the $(1\bar{2}0)$ plane for the scattering components from the second (open circles), and deeper layers (full circles) Ni atoms.

complete elimination of carbon contamination from the surface.

The sample was mounted on a six-axis goniometer and analyzed by MEIS using 120-keV He^+ ions. A high-resolution toroidal electrostatic analyzer makes it possible to obtain the scattering component from each atomic plane. The sample can be heated up to 700 K during the MEIS experiment with infrared radiation of a tungsten filament from the backside of the sample holder. He^+ irradiation introduces damage in the crystal and, in order to suppress it, the irradiated area was shifted after the integrated beam current of 0.5–1 μC. Details of the experimental set-up and data analysis procedure are described elsewhere.[10,16]

III. RESULTS AND DISCUSSION

Figure 1 shows the MEIS spectra for 120-keV He^+ ions incident along the [201] axis and $+1.0°$ off from this axis and backscattered from Ni atoms of NiO(001) at RT. Here, we must note that the rhombohedral NiO lattice is in good approximation regarded as a cubic one ($a=4.177$ Å, $\alpha=90°42'$ at RT). The surface peaks are deconvoluted into primary three scattering components from the top, second, and third layers, assuming symmetric Gaussian shapes. The energy difference between the neighboring components can be estimated from other clearly resolved surface peaks observed in the different scattering geometries [see, for example, Figs. 6(a) and 6(b)]. For the off-axis condition, the scattering yield from the second-layer Ni decreases but those from the third- and deeper layer Ni atoms increase. This indicates a vertical displacement of the top-layer O atoms. We observe the scattering yields from the second-, third-, and deeper layer atoms as a function of incident angle for various kinds of scattering geometries and derive the angles giving scattering yield minima for the above three scattering components. If the surface is relaxed but not reconstructed, the angles giving scattering yield minima for the second and deeper layers, respectively determine the interlayer distance between the top and second layer and the exact bulk crystal axis. In fact, clear 1×1 RHEED patterns indicate no surface reconstruction and scanning tunneling microscopy observation also guarantees the 1×1 surface.[3] In addition, it is quite reasonable to assume no relaxation for deeper layers than the fourth.

Figures 2(a) and 2(b) show the angular scan spectra for the second-, third-, and deeper layer Ni atoms around the [111] axis in the $(1\bar{1}0)$ plane and around the [211] axis in the $(1\bar{2}0)$ plane, respectively. Here, the emerging angle was fixed and the scattering yield was corrected taking account the scattering cross section depending on scattering angle. For the incidence along the [111] axis, the top-layer O atoms shadow the second-layer Ni atoms and the top-layer Ni and second-layer O atoms shadow the third-layer Ni atoms. A Monte Carlo simulation of ion trajectories shows that the top-layer Ni atoms dominate the hitting probability for the third-layer Ni atoms due to considerably strong interaction between He^+ ions and Ni atoms compared with that between He^+ and O. Thus the angular scan around the [111] axis for the scattering components from the second- and third-layer Ni atoms gives the interplanar distance between the top-layer O plane and second-layer Ni plane ($d_{1O\text{-}2N}$) and that between the top- and third-layer Ni plane ($d_{1N\text{-}3N}$), respectively. The angular scan around the [211] axis in the $(1\bar{2}0)$ plane for the scattering component from the second-layer Ni determines the interplanar distance between the top- and second-layer Ni plane ($d_{1N\text{-}2N}$). Furthermore, we perform the angular scan around the [201] axis in the (010) plane for the scattering component from the second-layer O atoms and obtain the interplanar distance between the top-layer Ni plane and the second-layer O plane ($d_{1N\text{-}2O}$). From the above analysis, the vertical positions of the top-layer O and Ni planes and of the second-layer O and Ni planes scaled

TABLE I. Surface relaxation ($\varepsilon_{i,j}$) and rumpling [$\Delta\varepsilon(i)$] for NiO(001) determined experimentally by present MEIS and LEED (Ref. 16) along with theoretical *ab initio* (Ref. 12) and shell model (Ref. 17) calculations.

	$\varepsilon_{1,2}$ (%)	$\varepsilon_{2,3}$ (%)	$\Delta\varepsilon(1)$ (%)	$\Delta\varepsilon(2)$ (%)
MEIS	-1.9 ± 0.6	$+0.5\pm0.8$	-4.8 ± 0.6	$+1.0\pm0.8$
LEED	-1.9	—	$-5\sim+5$	—
Ab initio	-1.4	-0.5	-2.5	-1.9
Shell model	-1.03	$+0.14$	$+10.20$	-0.15
MD	-1.51	$+0.25$	$+0.63$	-0.14

from the third-layer Ni plane are determined to be $2d_{bulk}-0.080\pm0.005$, $2d_{bulk}+0.021\pm0.005$, $d_{bulk}+0.022\pm0.005$, and $d_{bulk}+0.0\pm0.005$ Å, respectively [d_{bulk} is the bulk interplanar distance (2.0885 Å)]. The result obtained at RT is shown in Table I and compared with other experimental data[17] and theoretical predictions by the shell model[18] and *ab initio* calculation based on the local spin density approximation.[13] Here, the relaxation $\varepsilon_{i,i+1}$ between the ith and $(i+1)$th layers, and the rumpling $\Delta\varepsilon(i)$ of the ith layer are defined as

$$\varepsilon_{i,i+1}=\left(\frac{\sigma_{i,-}+\sigma_{i,+}}{2d_{bulk}}-\frac{\sigma_{i+1,-}+\sigma_{i+1,+}}{2d_{bulk}}\right)\times100(\%),$$

$$\Delta\varepsilon(i)=\left(\frac{\sigma_{i,-}-\sigma_{i,+}}{d_{bulk}}\right)\times100(\%), \quad (1)$$

where $\sigma_{i,-}$ and $\sigma_{i,+}$ are the displacements of the ith layer anion and cation from the bulk positions, respectively. The plus sign means a displacement toward the vacuum side. The present result shows that the interlayer distance between the top and second layers is significantly contracted. It agrees with the experimental and theoretical results by low energy electron diffraction (LEED),[17] the *ab initio* and shell model[18] calculations. It is also found that the top-layer Ni plane is displaced toward the vacuum side relative to the top-layer O plane. This result is consistent with the *ab initio* calculation but contradicts the shell model calculation using pair potentials. Small discrepancies between the MEIS and *ab initio* results are probably due to the fact that the *ab initio* calculation was made assuming the local spin density approximation at zero temperature.

A knowledge of the relaxation between the top- and second-layer rumpling together with the polarizability of O^{2-} (2.61×10^{-24} cm^3) and Ni^{2+} (0.05×10^{-24} cm^3) (Ref. 19) allows the self-consistent deduction of the dipole moments of the top- and second-layer O^{2-} and Ni^{2+} to be $+0.225$ (top-layer O^{2-}), -0.066 (top-layer Ni^{2+}), -0.017 (second-layer O^{2-}) and $+0.017$ (second-layer Ni^{2+}) in Debye units.[10] If one uses pair potentials, top-layer ions with a larger dipole moment are displaced toward the vacuum side relative to those with a smaller dipole moment. Thus the present MEIS result shows that pair potentials cannot reproduce the surface rumpling of NiO(001). Here, it must be noted that NiO crystal has both ionic and covalent natures and the ionic bonds are basically isotropic, while the covalent bonds are strongly directional. Therefore, it is reasonable to apply pair potentials to ionic crystals but not to covalent ones.

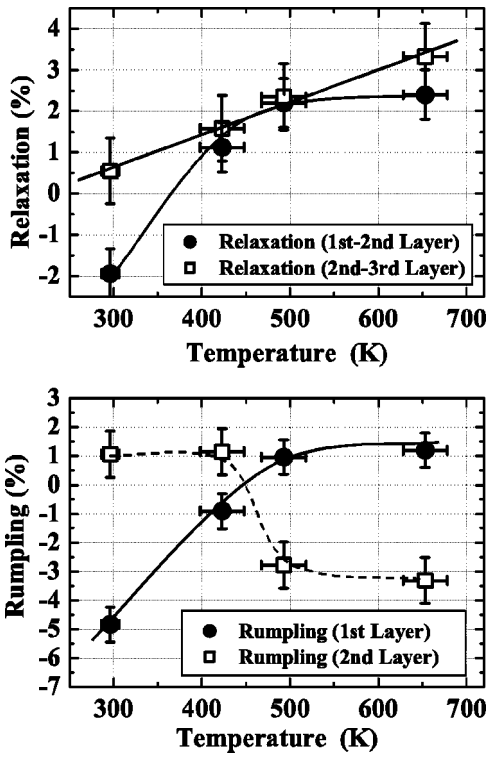

FIG. 3. (a) Relaxation between the top and second layer (full circles) and between the second and third layers (open squares) measured at RT, 420, 500, and 650 K. (b) Rumpling of the top (full circles) and second (open squares) layers measured at RT, 420, 500, and 650 K. Solid and dashed curves are drawn to guide the eye.

A similar analysis is performed at temperatures of 420, 500, and 650 K. Figures 3(a) and 3(b) indicate the temperature-dependent relaxation and rumpling determined by MEIS. Quite reasonably, the interlayer distances expand with increasing temperature. The relaxation between the top and second layers and the rumpling of the top layer rapidly vary with increasing temperature up to 500 K, while it is almost constant at higher temperatures. It is interesting that at a temperature above 500 K (close to the Néel temperature), the relative positions of the O plane to the Ni plane in the top and second layers are reversed. Such a temperature dependent behavior of the rumpling suggests that the surface structure is very sensitive to even a slight change of the bulk lattice, although it does not change the electronic band structure significantly. Here, it should be noted that the *ab initio* calculation is performed to determine the structure in the ground states, meaning at zero degree temperature and thus it does not always predict the surface structure at higher temperatures.

The TVAs of the top-layer atoms are enhanced pronouncedly in the surface normal direction (z-axis). According to the MD simulation and the result for alkali halide crystals,[9,10] the enhancement of the average TVAs of the top-layer atoms in the direction parallel to the surface [$\langle u(1,x)\rangle$] and of the second-layer atoms [$\langle u(2,x)\rangle$, $\langle u(2,z)\rangle$] is con-

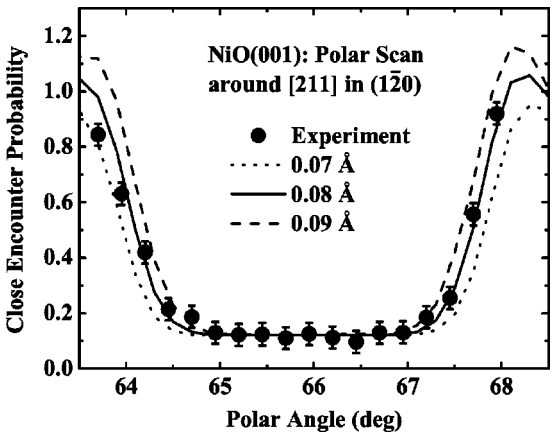

FIG. 4. Polar scan spectrum around the [211] axis in the $(1\bar{2}0)$ plane for scattering components mainly from the fifth- to seventh-layer Ni atoms. Dotted, solid, and dashed curves are obtained by a Monte Carlo simulation of ion trajectories assuming one dimensional rms TVAs of 0.07, 0.08, and 0.09 Å, respectively.

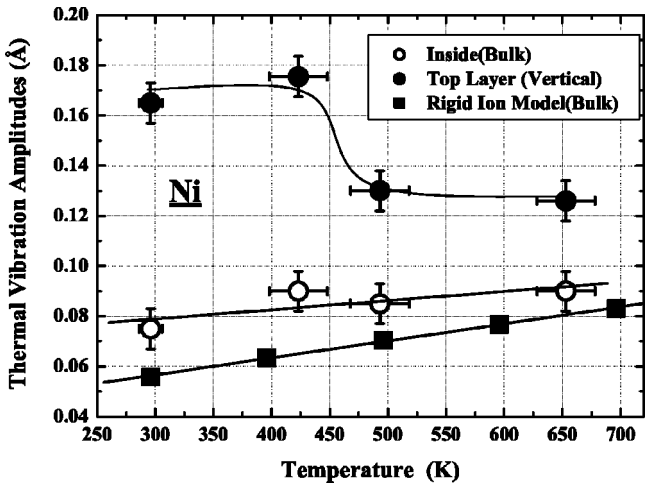

FIG. 5. One-dimensional rms TVAs for Ni atoms inside the NiO crystal (open circles) and those in the surface normal direction for top-layer Ni atoms (full circles) measured at RT, 420, 500, and 650 K. Full squares indicate the bulk TVAs calculated by the rigid ion model using the pair potential proposed by Lewis and Catlow (Ref. 22).

siderably smaller than that of the top-layer atoms in the normal direction [$\langle u(1,z)\rangle$]. Thus as a first approximation, the enhancement is neglected except for $\langle u(1,z)\rangle$. Figure 4 shows the angular scan spectrum observed at RT around the [211] axis in the $(1\bar{2}0)$ plane for the scattering component mainly from fifth- to seventh-layer Ni atoms. It must be noted that the [211] string consists of only either Ni or O atoms. The polar scan profile for the scattering components from deep layer atoms depends on the bulk TVAs but not significantly on the correlations and enhancements of TVAs for near-surface atoms.[10] The hitting probability for each layer atom is calculated by Monte Carlo simulation of ion trajectories assuming the bulk TVAs. The observed angular scan spectrum is reproduced well assuming the one-dimensional bulk TVA (Ni) of 0.076 ± 0.005 Å. This value coincides well with the previously determined value of 0.075 ± 0.005 Å by angular scan around the [101] axis.[12] One may expect that a similar angular scan for the scattering component from deep layers of O atoms would lead to the determination of the bulk TVA of O. Unfortunately, however, it is quite difficult to obtain a reliable angular scan spectrum for O because of the overlapping high background level from deep layers of Ni.

If one assumes that an enhancement of TVAs occurs only for the top-layer atoms in the surface normal direction, the $\langle u(1,x)\rangle$ and $\langle u(1,z)\rangle$ values are deduced from the scattering yield from the second-layer Ni atoms normalized by that from the top-layer Ni atoms (normalized hitting probability). Here, let us define the enhancement (β) of the TVA of the top-layer atoms in the normal direction as $\langle u(1,z)\rangle = \beta\langle u(1,x)\rangle$. In the previous study,[10] the normal and lateral components of the TVAs were determined to be 0.084 ± 0.003 Å [$\langle u_{Ni}(1,x)\rangle$] and 1.90 ± 0.05 (β_{Ni}) for Ni and 0.078 ± 0.003 Å [$\langle u_O(1,x)\rangle$] and 1.20 ± 0.05 (β_O) for O. These values were deduced from the normalized hitting probabilities for the second-layer Ni atoms observed for [101] and [211] incidence and from those observed for [111] and [221] incidence. The $\langle u_{Ni}(1,x)\rangle$ value of 0.084 Å means a slight enhancement (10%) of the TVA in the lateral direction for the top-layer Ni. This result supports the validity of the assumption that $\langle u(1,x)\rangle$ is approximated to be the one-dimensional bulk TVA. If one uses this assumption, one can estimate the Debye temperature to give the bulk TVA averaged for Ni and O [$(0.076+0.078)/2=0.077$ Å]. Here, we employ the Debye approximation which gives one-dimensional rms TVA at temperature T K. It is expressed by the following relationship valid for monatomic solids:

$$\langle u_1^2\rangle = \frac{3}{M\omega_D^3}\int_0^{\omega_D}\omega\hbar\left\{\frac{1}{\exp(\omega\hbar/k_BT)-1}+1/2\right\}d\omega, \quad (2)$$

where M, ω_D, $\hbar$, and k_B are the atomic mass, the Debye cutoff frequency, and the Planck and Boltzmann constants, respectively. The ω_D value is given by the Debye temperatures Θ ($\omega_D\hbar=k_B\Theta$). The Debye temperature is derived to be 554 K, which is significantly larger than that (390 K) estimated from the elastic constants.[20] If one applies the above Debye approximation assuming appropriate Debye temperature for Ni (Θ_{Ni}) and O (Θ_{O}) separately to give the $\langle u_{Ni}(bulk)\rangle$ of 0.076 Å and the $\langle u_O(bulk)\rangle$ of 0.078 Å, one obtains $\Theta_{\mathrm{Ni}}=366$ K and $\Theta_{\mathrm{O}}=719$ K. From heat capacity measurements, it has been reported that the Θ_{Ni} and Θ_{O} values, respectively are 425 and 900 K (Ref. 21) and 515.9 and 762.5 K.[22] The agreement between the present MEIS and heat capacity results seems relatively good.

Temperature dependences of the bulk and enhanced TVAs for Ni are depicted in Fig. 5. The bulk TVA gradually increases with increasing temperature. Its temperature dependence is almost consistent with that calculated from the rigid ion model using the Lewis-Catlow pair potential[23] but the absolute TVA values determined by MEIS are 15–25 % larger than the calculated ones. As mentioned in the literature,[23] the expression of the pair potential is not very reliable because of many potential parameters and lack of

experimental data. In contrast to the bulk TVAs, the enhancement of the TVA of the top-layer Ni in surface normal direction suddenly drops at a temperature above 500 K. This may be due to the fact that the distance between the top-layer Ni atoms and the underlying O atoms is almost equal to the bulk interplanar distance at RT and 420 K but expanded by 0.06–0.07 Å at 500 and 650 K. At temperature above 500 K, the top-layer Ni plane takes the downward position relative to the O plane [see Fig. 3(b)]. The MD simulation using a pair potential predicts a pronounced enhancement of the top-layer atoms taking an upper plane in the surface normal direction. In fact, at RT the enhancement of the top-layer O atoms is relatively small ($\beta_O = 1.20 \pm 0.05$), which take a downward position relative to the top-layer Ni atoms. Thus, the reversal of the top-layer rumpling may change dramatically the enhancement of the TVAs of the top-layer atoms in the normal direction. Unfortunately, the enhancement of the top-layer O atoms at higher temperatures could not be determined by MEIS, because of increased uncertainties in deconvoluting the MEIS spectra from the He ions passing through the top-layer O atoms.

If one employs the approximation that the TVAs are independent of depth except for the enhancement of the top-layer atoms, one can determine the correlations of thermal vibrations between the nearest neighbor atoms for a major crystal string. In the discussion made so far, the effect of correlated thermal vibrations is neglected, because the higher the Miller index the smaller the correlations. In fact, our previous work on the lattice dynamics of alkali halide crystals showed that the correlations between the nearest neighbor atoms in the [001] and [101] strings are significant but small enough for the [111] string.[10,11] Here, the correlation coefficient is defined by

$$C^{A-B} = \frac{\langle u_A \cdot u_B \rangle}{\sqrt{\langle u_A^2 \rangle \langle u_B^2 \rangle}}, \tag{3}$$

where u_A and u_B are the displacements of atoms A and B from their equilibrium positions, respectively. We measured the MEIS spectrum for 120-keV He^+ ions incident along the [001] axis and backscattered to the [601] direction [Fig. 6(a)]. Decomposing the MEIS spectrum into the scattering component from each atomic layer deduces a normalized hitting probability of 0.43 for the second-layer Ni atoms in the [001] string. As a first approximation, we assume that the TVAs of the second-layer atoms are the same as those of the bulk and calculate the hitting probability for the second-layer Ni atoms considering the correlation coefficient by Monte Carlo simulation of ion trajectories based on the binary collision model.[10,11] Here, the correlations are taken into account only for the nearest neighbor atoms and the lateral and vertical TVAs of the top-layer O and Ni atoms are already known. The correlation coefficient giving the normalized hitting probability of 0.43 is just the solution. Thus we obtain a correlation coefficient ($C_{001}^{O\text{-}Ni}$) of 0.0 ± 0.1, namely no correlations between the top-layer O and the second-layer Ni atoms in the [001] string for the motion perpendicular to the [001] axis. Figure 6(b) shows the MEIS spectrum observed for 120-keV He^+ ions incident along the [101] axis and backscattered to 80° (random direction) in the (010) plane. The normalized hitting probability for the second-layer Ni atoms is deduced to be 0.42. It gives the correlation coefficient of ($C_{101}^{Ni\text{-}Ni}$) -0.05 ± 0.1 between the top- and second-layer Ni atoms in the [101] string for the motion perpendicular to the [101] axis. Previously, we neglected the correlation for the [101] incidence to extract the $\langle u_{Ni}(1,x) \rangle$ and $\langle u_{Ni}(1,z) \rangle$ values. Now, it is seen that this assumption is adequate. The MD simulation using the Lewis-Catlow pair potential gives strong correlations between the first nearest neighbor atoms in the [001] and [101] strings for the motion perpendicular to each crystal axis ($C_{001}^{O\text{-}Ni} = +0.36 \pm 0.08$ and $C_{101}^{Ni\text{-}Ni} = +0.29 \pm 0.08$). In general, pair potentials applied to NaCl-type crystal surfaces lead to strong positive correlations between the first nearest neighbor atoms in the [001] and [101] strings. The present result on the correlation of lattice vibrations also indicates that any potentials are not applicable to the NiO crystal.

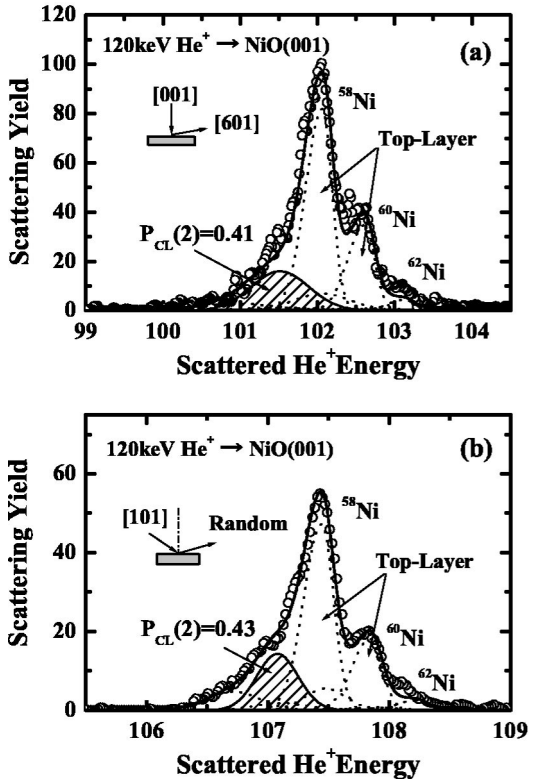

FIG. 6. (a) MEIS spectrum from Ni observed for 120-keV He^+ ions incident along the [001] axis and backscattered to the [601] direction. Thick solid and dashed curves are best-fitted total and decomposed spectra from the top layer, respectively. The shaded spectrum indicates the deconvoluted scattering component from the second-layer Ni. (b) MEIS spectrum from Ni for [101] incidence and random emergence (scattering angle: 80°). The shaded spectrum is the deconvoluted scattering component from the second-layer Ni.

IV. CONCLUSION

A high-resolution MEIS analysis determined the vertical positions of the top-layer O and Ni planes and of the second-

layer O and Ni planes scaled from the third-layer Ni plane. The present result shows that the interlayer distance between the top and second layers is significantly contracted. It agrees with the experimental and theoretical results by LEED, *ab initio* methods and shell model calculations. It is also found that the top-layer Ni plane is displaced toward the vacuum side relative to the top-layer O plane at temperatures below 420 K. This result is consistent with the *ab initio* calculation but contradicts the shell model calculation using pair potentials. The treatment using any pair potentials cannot explain the upward displacement of the top-layer ions with a smaller dipole moment relative to those with a larger dipole moment. It is noteworthy that the top-layer ions with a larger dipole moment take an upper position for alkali halide crystal surfaces.[10,11] The NiO crystal has both ionic and covalent natures. The ionic bonds are basically isotropic, while the covalent bonds are strongly directional. Thus it is quite reasonable that pair potentials are applicable to ionic crystals but not to covalent ones. At temperatures above 500 K (close to the Néel temperature), however, the relative positions of the O plane to the Ni plane in the top and second layers are reversed. Such a behavior suggests that the surface structure is very sensitive to even a slight change of the bulk lattice, although it does not change significantly the electronic band structure.

Temperature-dependent bulk and enhanced TVAs were also measured for Ni atoms. The Debye temperatures for Ni and O estimated from the bulk TVAs of Ni and O assuming the simple Debye model are consistent with those derived from the heat capacity measurement. The bulk TVA gradually increases with increasing temperature, while the enhancement of the TVA of the top-layer Ni in the surface normal direction suddenly drops at temperature above 500 K. Such a dramatic change is probably due to the fact that the top-layer N plane takes a lower position relative to the top-layer O plane above 500 K. In contrast to alkali halide crystals, no correlations were found between the first nearest neighbor atoms in the [001] and [101] strings for the motion perpendicular to the [001] and [101] axes. In general, pair potentials applied to NaCl-type crystals surfaces lead to strong positive correlations between the first nearest neighbor atoms in the [001] and [101] strings. Thus the above result also shows that pair potentials are not applicable to the NiO crystal which has in part covalent bonding.

ACKNOWLEDGMENTS

The authors would like to thank Y. Hoshino for his support in carrying out the MEIS experiment. Thanks are also due to I. Kato for his assistance in the MEIS data analysis.

*Corresponding author. Email address: ykido@se.ritsumei.ac.jp

[1] G.A. Sawatzky and J.W. Allen, Phys. Rev. Lett. **53**, 2339 (1984).
[2] D. Alders, F.C. Voogt, T. Hibma, and G.A. Sawatzky, Phys. Rev. B **54**, 7716 (1996).
[3] M.R. Castell, P.L. Wincott, N.G. Condon, C. Muggelberg, G. Thornton, S.L. Dudarev, A.P. Sutton, and G.A.D. Briggs, Phys. Rev. B **55**, 7859 (1997).
[4] D. Alders, L.H. Tjeng, F.C. Voogt, T. Hibma, G.A. Sawatzky, C.T. Chen, J. Vogel, M. Sacchi, and S. Iacobucci, Phys. Rev. B **57**, 11623 (1998).
[5] M. Marynowski, W. Franzen, M. El-Batanouny, and V. Staemmler, Phys. Rev. B **60**, 6053 (1999).
[6] M. Portalupi, L. Duò, G. Isella, R. Bertacco, M. Marcon, and F. Ciccacci, Phys. Rev. B **64**, 165402 (2001).
[7] S.L. Dudarev, A.I. Liechtenstein, M.R. Castell, G.A. Briggs, and A.P. Sutton, Phys. Rev. B **56**, 4900 (1997).
[8] S. Baroni, S. de Gironcoli, A.D. Corso, and P. Giannozzi, Rev. Mod. Phys. **73**, 515 (2001).
[9] E.M.L. Chung, D.M.K. Paul, G. Balakrishnan, M.R. Lees, A. Ivanov, and M. Yethiraj, Phys. Rev. B **68**, 140406(R) (2003).
[10] T. Okazawa, T. Nishimura, and Y. Kido, Phys. Rev. B **66**, 125402 (2002).
[11] Y. Kido and T. Okazawa, Surf. Rev. Lett. **10**, 389 (2003).
[12] T. Okazawa, Y. Yagi, and Y. Kido, Phys. Rev. B **67**, 195406 (2003).
[13] H. Momida and T. Oguchi, J. Phys. Soc. Jpn. **72**, 588 (2003).
[14] J.A. Hofmann, A. Paskin, K. Tauer, and R.J. Weiss, J. Phys. Chem. Solids **1**, 45 (1956).
[15] M. Marynowski, W. Franzen, M. El-Batanouny, and V. Staemmler, Phys. Rev. B **60**, 6053 (1999).
[16] T. Nishimura, A. Ikeda, and Y. Kido, Rev. Sci. Instrum. **69**, 1671 (1998).
[17] M.R. Welton-Cook and M. Prutton, J. Phys. C **13**, 3993 (1980).
[18] H. Nakatsugawa and E. Iguchi, Surf. Sci. **357-358**, 96 (1996).
[19] R.R. Reddy, Y.N. Ahammed, P.A. Azeem, K.R. Gopal, and T.V.R. Rao, J. Non-Cryst. Solids **286**, 169 (2001).
[20] Y. Noguchi, M. Uchino, H. Hikosaka, T. Atou, K. Kusaba, K. Fukuoka, T. Mashimo, and Y. Syono, J. Phys. Chem. Solids **60**, 509 (1999).
[21] J.A. Hoffmann, A. Paskin, K.J. Tauer, and R.J. Weiss, J. Phys. Chem. Solids **1**, 45 (1956).
[22] B. Bergman and J. Å gren, J. Am. Ceram. Soc. **68**, 444 (1985).
[23] G.V. Lewis and C.R.A. Catlow, J. Phys. C **18**, 1149 (1985).